Nonparaxial propagation of a super-Lorentz–Gauss SLG_{01} mode beam*

Zhou Guo-Quan(周国泉)†

School of Sciences, Zhejiang Forestry University, Lin'an 311300, *Zhejiang Province, China*

(Received 22 September 2009; revised manuscript received 4 November 2009)

Based on the vectorial Rayleigh–Sommerfeld integral formulae, this paper derives the analytical nonparaxial propagation equation of a super-Lorentz–Gauss (SLG) SLG_{01} mode beam in free space. The far field expression and the scalar paraxial result are treated with special cases of the general formulae. According to the obtained analytical representation, the nonparaxial propagation properties of the SLG_{01} mode beam are illustrated and analysed with numerical examples. This research provides an approach to investigate the propagation of the SLG_{01} mode beam within the framework of the nonparaxial regime.

Keywords: vectorial Rayleigh–Sommerfeld integral, super-Lorentzian–Gauss beam, nonparaxial propagation

PACC: 4225B, 4260H

1. Introduction

With the same spatial extension, the angular spreading of a Lorentz–Gaussian distribution is higher than that of a Gaussian description.[1] Therefore, the Lorentz–Gauss beam provides an appropriate model to describe highly divergent beams.[2,3] The Lorentz beam is a special case of Lorentz–Gauss beams. The paraxial propagation of Lorentz–Gauss and Lorentz beams in free space has been investigated.[2] The vectorial structural property of a Lorentz–Gauss beam has been examined in the far field.[4] On the basis of the vectorial Rayleigh–Sommerfeld integral formulae, analytical propagation equations of Lorentz–Gauss and off-axis Lorentz beams beyond the paraxial approximation have been derived.[5,6] The focal shift of a Lorentz–Gauss beam focused by an aperture-lens system has been numerically investigated.[7] The fractional Fourier transform has been applied to deal with the propagation of a Lorentz beam.[8] The outcome of a finite linear combination of Lorentz beams is a super-Lorentzian beam.[9] Based on second-order moments, the beam propagation factor of a paraxial Lorentz beam is verified to be $\sqrt{2}$,[10] and the beam propagation factor of a paraxial Lorentz–Gauss beam is between 1 and $\sqrt{2}$.[11] As a result, Lorentz–Gauss and Lorentz beams are only valid for the description of fundamental mode beams with high divergence. Therefore, an orthonormal family of super-Lorentz–Gauss (SLG) beam has been introduced to describe high-order mode beams with high divergence.[12] The lowest-order SLG beam is the SLG_{00} mode beam, which is just the Lorentz–Gauss beam. The first-order SLG beams are the SLG_{01} and SLG_{10} mode beams. As to the SLG_{10} mode beam, it can be obtained by exchange of x and y in the field expression of the SLG_{01} mode beam. Here, we mainly pay attention to the SLG_{01} mode beam. As the physical picture of SLG beams is similar to that of Hermite–Gaussian (HG) beams, HG beams are chosen as the comparative object. According to the beam order, the SLG_{01} mode beam corresponds to the HG_{01} mode beam. In the paraxial case, the divergence of the SLG_{01} mode beam is verified to be larger than that of the corresponding HG_{01} mode beam.[12] Accordingly, the SLG_{01} mode beam is more appropriate than the HG_{01} mode beam to describe the first-order mode beams with high divergence. However, the paraxial approximation is invalid for beams with a large divergent angle. In this case, a nonparaxial model is in order. Therefore, the nonparaxial propagation of the SLG_{01} mode beam is investigated in this paper. Many approaches have been proposed to deal with the nonparaxial propagation of laser beams,[13–16] and the vectorial Rayleigh–Sommerfeld integral method is a suitable one.[17,18] In the present paper, the description of the SLG_{01} mode beam is directly derived from the vectorial Rayleigh–Sommerfeld integral formulae.

*Project supported by the National Natural Science Foundation of China (Grant No. 10974179) and the Natural Science Foundation of Zhejiang Province of China (Grant No. Y1090073).

†Corresponding author. E-mail: zhouguoquan178@sohu.com

© 2010 Chinese Physical Society and IOP Publishing Ltd

2. Nonparaxial propagation of the SLG_{01} mode beam

In the Cartesian coordinate system, the z-axis is taken to be the propagation axis. The SLG_{01} mode beam in the source plane z=0 is described by[12]

$$\begin{pmatrix} E_x(x_0, y_0, 0) \\ E_y(x_0, y_0, 0) \end{pmatrix} = \begin{pmatrix} \dfrac{2w_{0x}\sqrt{w_{0x}w_{0y}}}{\pi} \dfrac{y_0}{(x_0^2 + w_{0x}^2)(y_0^2 + w_{0y}^2)} \exp\left(\dfrac{\mathrm{i}\, k\rho_0^2}{2q_0}\right) \\ 0 \end{pmatrix}, \tag{1}$$

where $\rho_0 = (x_0^2 + y_0^2)^{1/2}$, w_{0x} and w_{0y} are parameters related to the beam widths of the super-Lorentzian part in the x- and y-directions, respectively, $k = 2\pi/\lambda$ with λ being the wavelength, $q_0 = -\mathrm{i}\, k w_0^2/2$ is the beam q parameter in the source plane, w_0 is the waist of the Gaussian part. The time-dependent factor $\exp(-\mathrm{i}\,\omega t)$ is omitted in Eq. (1), and ω is the circular frequency. By means of the vectorial Rayleigh–Sommerfeld integral formulae, the SLG_{01} mode beam propagating toward half free space $z > 0$ is found to be[17]

$$E_x(\boldsymbol{r}) = -\frac{1}{2\pi} \int_{-\infty}^{\infty} \int_{-\infty}^{\infty} E_x(x_0, y_0, 0) \frac{\partial \boldsymbol{G}(\boldsymbol{r}, \boldsymbol{\rho}_0)}{\partial z} \mathrm{d}x_0 \mathrm{d}y_0, \tag{2}$$

$$E_y(\boldsymbol{r}) = -\frac{1}{2\pi} \int_{-\infty}^{\infty} \int_{-\infty}^{\infty} E_y(x_0, y_0, 0) \frac{\partial \boldsymbol{G}(\boldsymbol{r}, \boldsymbol{\rho}_0)}{\partial z} \mathrm{d}x_0 \mathrm{d}y_0, \tag{3}$$

$$E_z(\boldsymbol{r}) = \frac{1}{2\pi} \int_{-\infty}^{\infty} \int_{-\infty}^{\infty} \left(E_x(x_0, y_0, 0) \frac{\partial \boldsymbol{G}(\boldsymbol{r}, \boldsymbol{\rho}_0)}{\partial x} + E_y(x_0, y_0, 0) \frac{\partial \boldsymbol{G}(\boldsymbol{r}, \boldsymbol{\rho}_0)}{\partial y} \right) \mathrm{d}x_0 \mathrm{d}y_0 \tag{4}$$

with $\boldsymbol{G}(\boldsymbol{r}, \boldsymbol{\rho}_0)$ given by

$$\boldsymbol{G}(\boldsymbol{r}, \boldsymbol{\rho}_0) = \frac{\exp(\mathrm{i}\, k\, |\boldsymbol{r} - \boldsymbol{\rho}_0|)}{|\boldsymbol{r} - \boldsymbol{\rho}_0|}, \tag{5}$$

where $\boldsymbol{r} = x\boldsymbol{i} + y\boldsymbol{j} + z\boldsymbol{k}$, and $\boldsymbol{\rho}_0 = x_0\boldsymbol{i} + y_0\boldsymbol{j}$. The $\boldsymbol{i}$, $\boldsymbol{j}$ and $\boldsymbol{k}$ are the three unit base vectors. The following approximation is valid beyond the paraxial approximation[19,20]

$$\boldsymbol{G}(\boldsymbol{r}, \boldsymbol{\rho}_0) = \frac{1}{r} \exp\left[\mathrm{i}\, k \left(r + \frac{\rho_0^2 - 2xx_0 - 2yy_0}{2r} \right) \right], \tag{6}$$

where $r = (x^2 + y^2 + z^2)^{1/2}$. Inserting Eqs. (1) and (6) into Eqs. (2)–(4), we obtain the propagating SLG_{01} mode beam as

$$E_x(\boldsymbol{r}) = \frac{-\mathrm{i}\, 2z w_{0x}\sqrt{w_{0x}w_{0y}}}{\pi\lambda r^2} \exp(\mathrm{i}\, kr) T_1(x, z) T_2(y, z), \tag{7}$$

$$E_y(\boldsymbol{r}) = 0, \tag{8}$$

$$E_z(\boldsymbol{r}) = \frac{\mathrm{i}\, 2w_{0x}\sqrt{w_{0x}w_{0y}}}{\pi\lambda r^2} \exp(\mathrm{i}\, kr)[xT_1(x, z) - T_2(x, z)] T_2(y, z) \tag{9}$$

with $T_1(j, z)$ and $T_2(j, z)$ given by

$$T_1(j, z) = \exp\left(-\frac{\mathrm{i}\, kj^2}{2Ar}\right) \int_{-\infty}^{\infty} \frac{1}{j_0^2 + w_{0j}^2} \exp\left[\frac{\mathrm{i}\, kA}{2r} \left(\frac{j}{A} - j_0 \right)^2 \right] \mathrm{d}j_0, \tag{10}$$

$$T_2(j, z) = \exp\left(-\frac{\mathrm{i}\, kj^2}{2Ar}\right) \int_{-\infty}^{\infty} \frac{j_0}{j_0^2 + w_{0j}^2} \exp\left[\frac{\mathrm{i}\, kA}{2r} \left(\frac{j}{A} - j_0 \right)^2 \right] \mathrm{d}j_0, \tag{11}$$

where $j = x$ or y (hereafter), and $A = 1 + r/q_0$. We note that the convolution of two functions $f_1(\tau)$ and $f_2(\tau)$ is defined by

$$f_1(\tau) * f_2(\tau) = \int_{-\infty}^{\infty} f_1(\eta) f_2(\tau - \eta) \mathrm{d}\eta, \tag{12}$$

where the asterisk denotes the convolution. Equations (10) and (11) can be rewritten in convolution form as

$$T_1(j,z) = \exp\left(-\frac{\mathrm{i}\,kj^2}{2Ar}\right)\left[f_1\left(\frac{j}{A}\right) * f_2\left(\frac{j}{A}\right)\right], \quad (13)$$

$$T_2(j,z) = \exp\left(-\frac{\mathrm{i}\,kj^2}{2Ar}\right)\left[f_3\left(\frac{j}{A}\right) * f_2\left(\frac{j}{A}\right)\right], \quad (14)$$

where the auxiliary functions $f_1(\tau)$, $f_2(\tau)$, and $f_3(\tau)$ are separately given by

$$f_1(\tau) = \frac{1}{w_{0j}^2 + \tau^2}, \quad (15)$$

$$f_2(\tau) = \exp\left(\frac{\mathrm{i}\,kA}{2r}\tau^2\right), \quad (16)$$

$$f_3(\tau) = \frac{\tau}{w_{0j}^2 + \tau^2}. \quad (17)$$

The corresponding Fourier transforms of $f_1(\tau)$, $f_2(\tau)$, and $f_3(\tau)$ are given by

$$\begin{aligned} f_1(\xi) &= \frac{1}{\sqrt{2\pi}}\int_{-\infty}^{\infty}\frac{1}{w_{0j}^2+\tau^2}\exp(\mathrm{i}\,\xi\tau)\mathrm{d}\tau \\ &= \sqrt{\frac{\pi}{2}}\frac{1}{w_{0j}}\exp(-w_{0j}\,|\xi|), \end{aligned} \quad (18)$$

$$\begin{aligned} f_2(\xi) &= \frac{1}{\sqrt{2\pi}}\int_{-\infty}^{\infty}\exp\left(\frac{\mathrm{i}\,kA}{2r}\tau^2\right)\exp(\mathrm{i}\,\xi\tau)\mathrm{d}\tau \\ &= \sqrt{\frac{\mathrm{i}\,r}{kA}}\exp\left(-\frac{\mathrm{i}\,r\xi^2}{2kA}\right), \end{aligned} \quad (19)$$

$$\begin{aligned} f_3(\xi) &= \frac{1}{\sqrt{2\pi}}\int_{-\infty}^{\infty}\frac{\tau}{w_{0j}^2+\tau^2}\exp(\mathrm{i}\,\xi\tau)\mathrm{d}\tau \\ &= \mathrm{i}\sqrt{\frac{\pi}{2}}\frac{|\xi|}{\xi}\exp(-w_{0j}\,|\xi|). \end{aligned} \quad (20)$$

The convolution theorem of the Fourier transform has[21]

$$f_1(\tau) * f_2(\tau) = \int_{-\infty}^{\infty} f_1(\xi)f_2(\xi)\exp(-\mathrm{i}\,\xi\tau)\mathrm{d}\xi. \quad (21)$$

Therefore, equations (13) and (14) turn out to be

$$\begin{aligned} T_1(j,z) = {} & \frac{1}{w_{0j}}\sqrt{\frac{\mathrm{i}\,\pi r}{2kA}}\exp\left(-\frac{\mathrm{i}\,kj^2}{2Ar}\right)\left\{\int_0^{\infty}\exp\left[-\frac{\mathrm{i}\,r\xi^2}{2kA}-\left(w_{0j}+\mathrm{i}\,\frac{j}{A}\right)\xi\right]\mathrm{d}\xi\right. \\ & \left.+\int_0^{\infty}\exp\left[-\frac{\mathrm{i}\,r\xi^2}{2kA}-\left(w_{0j}-\mathrm{i}\,\frac{j}{A}\right)\xi\right]\mathrm{d}\xi\right\}, \end{aligned} \quad (22)$$

$$\begin{aligned} T_2(j,z) = {} & \mathrm{i}\sqrt{\frac{\mathrm{i}\,\pi r}{2kA}}\exp\left(-\frac{\mathrm{i}\,kj^2}{2A}\right)\left\{\int_0^{\infty}\exp\left[-\frac{\mathrm{i}\,r\xi^2}{2kA}-\left(w_{0j}+\mathrm{i}\,\frac{j}{A}\right)\xi\right]\mathrm{d}\xi\right. \\ & \left.-\int_0^{\infty}\exp\left[-\frac{\mathrm{i}\,r\xi^2}{2kA}-\left(w_{0j}-\mathrm{i}\,\frac{j}{A}\right)\xi\right]\mathrm{d}\xi\right\}. \end{aligned} \quad (23)$$

By performing the integrals, from Eqs. (22) and (23) we obtain

$$T_1(j,z) = \frac{\pi}{2w_{0j}}\exp\left(-\frac{\mathrm{i}\,kj^2}{2Ar}\right)[V_j^+(j,z)+V_j^-(j,z)], \quad (24)$$

$$T_2(j,z) = \mathrm{i}\,\frac{\pi}{2}\exp\left(-\frac{\mathrm{i}\,kj^2}{2Ar}\right)[V_j^+(j,z)-V_j^-(j,z)] \quad (25)$$

with $V_j^{\pm}(j,z)$ given by

$$V_j^{\pm}(j,z) = \exp\left[\frac{kA}{2\,\mathrm{i}\,r}\left(w_{0j}\pm\mathrm{i}\,\frac{j}{A}\right)^2\right]\mathrm{erfc}\left[\sqrt{\frac{kA}{2\,\mathrm{i}\,r}}\left(w_{0j}\pm\mathrm{i}\,\frac{j}{A}\right)\right], \quad (26)$$

where

$$\mathrm{erfc}(x) = \frac{2}{\sqrt{\pi}}\int_x^{\infty}\exp(-s^2)\mathrm{d}s \quad (27)$$

is the complementary error function. Therefore, the analytical nonparaxial equation of the SLG_{01} mode beam is found to be

$$E_x(\boldsymbol{r}) = \frac{kz\sqrt{w_{0x}w_{0y}}}{4r^2}[V_x^+(x,z)+V_x^-(x,z)][V_y^+(y,z)-V_y^-(y,z)]\exp\left(-\frac{\rho^2}{w^2(r)}\right)\exp\left[\mathrm{i}\left(kr-\frac{z_r\rho^2}{rw^2(r)}\right)\right], \quad (28)$$

$$\begin{aligned} E_z(\boldsymbol{r}) = {} & -\frac{k\sqrt{w_{0x}w_{0y}}}{4r^2}[(x-\mathrm{i}\,w_{0x})V_x^+(x,z)+(x+\mathrm{i}\,w_{0x})V_x^-(x,z)][V_y^+(y,z)-V_y^-(y,z)] \\ & \times\exp\left(-\frac{\rho^2}{w^2(r)}\right)\exp\left[\mathrm{i}\left(kr-\frac{z_r\rho^2}{rw^2(r)}\right)\right], \end{aligned} \quad (29)$$

where $\rho = (x^2 + y^2)^{1/2}$, $w(r) = w_0(1 + r^2/z_r^2)^{1/2}$ is the beam radius of the Gaussian part, and $z_r = kw_0^2/2$. Now, we compare the nonparaxial propagation equation of the SLG_{01} mode beam with that of the SLG_{00} mode beam, which has been reported in Ref. [5]. The main difference is that their nonparaxial field expressions in the y-direction are different. For the SLG_{01} mode beam, there is a minus between $V_y^+(y,z)$ and $V_y^-(y,z)$, while for the SLG_{00} mode beam, there is a plus between $V_y^+(y,z)$ and $V_y^-(y,z)$. However, the nonparaxial field expressions of the SLG_{00} and SLG_{01} mode beams are identical in the x-direction.

The far field and paraxial expressions of the SLG_{01} mode beam can be also obtained under the far field and paraxial approximation conditions. In the far field regime, equation (6) can be further simplified to be

$$\boldsymbol{G}(\boldsymbol{r}, \boldsymbol{\rho}_0) = \frac{1}{r} \exp\left[\mathrm{i}\, k \left(r - \frac{xx_0 + yy_0}{r}\right)\right]. \tag{30}$$

As a result, the far field distribution of the SLG_{01} mode beam turns out to be

$$\begin{aligned} E_x(\boldsymbol{r}) = {} & \frac{kz\sqrt{w_{0x}w_{0y}}}{4r^2} \exp\left(\frac{f^2}{f_x^2} + \frac{f^2}{f_y^2}\right) \left[\exp\left(\frac{x}{f_x r}\right) \mathrm{erfc}\left(\frac{f}{f_x} + \frac{x}{2fr}\right) + \exp\left(-\frac{x}{f_x r}\right) \mathrm{erfc}\left(\frac{f}{f_x} - \frac{x}{2fr}\right)\right] \\ & \times \left[\exp\left(\frac{y}{f_y r}\right) \mathrm{erfc}\left(\frac{f}{f_y} + \frac{y}{2fr}\right) - \exp\left(-\frac{y}{f_y r}\right) \mathrm{erfc}\left(\frac{f}{f_y} - \frac{y}{2fr}\right)\right] \exp(\mathrm{i}\, kr), \end{aligned} \tag{31}$$

$$\begin{aligned} E_z(\boldsymbol{r}) = {} & -\frac{k\sqrt{w_{0x}w_{0y}}}{4r^2} \exp\left(\frac{f^2}{f_x^2} + \frac{f^2}{f_y^2}\right) \left\{(x - \mathrm{i}\, w_{0x}) \exp\left(\frac{x}{f_x r}\right) \mathrm{erfc}\left(\frac{f}{f_x} + \frac{x}{2fr}\right)\right. \\ & \left. + (x + \mathrm{i}\, w_{0x}) \exp\left(-\frac{x}{f_x r}\right) \mathrm{erfc}\left(\frac{f}{f_x} - \frac{x}{2fr}\right)\right\} \\ & \times \left\{\exp\left(-\frac{y}{f_y r}\right) \mathrm{erfc}\left(\frac{f}{f_y} - \frac{y}{2fr}\right) - \exp\left(\frac{y}{f_y r}\right) \mathrm{erfc}\left(\frac{f}{f_y} + \frac{y}{2fr}\right)\right\} \exp(\mathrm{i}\, kr), \end{aligned} \tag{32}$$

where

$$f = 1/kw_0, \quad f_x = 1/kw_{0x}, \quad f_y = 1/kw_{0y}, \tag{33}$$

are the f-parameters. The parameter f is a measure of the relative spot size of the Gaussian part w_0/λ. If w_0/λ is much larger than 1, the paraxial approximation is allowable for the Gaussian part; otherwise the nonparaxial correction of the Gaussian part should be taken into consideration. The parameters f_x and f_y are the measures of the relative spot size of the super-Lorentzian part in the x- and y-directions w_{0x}/λ and w_{0y}/λ, respectively. If w_{0x}/λ and w_{0y}/λ are much larger than 1, the paraxial approximation is permissible for the super-Lorentzian part; otherwise the nonparaxial correction of the super-Lorentzian part should be taken into account.

The propagation equation of the SLG_{01} mode beam in the paraxial regime can be treated as a special case by using the paraxial approximation

$$r = z + \frac{\rho^2}{2z} = z. \tag{34}$$

Accordingly, the paraxial SLG_{01} mode beam yields

$$\begin{aligned} E_x(\boldsymbol{r}) = {} & \frac{k\sqrt{w_{0x}w_{0y}}}{4z} \exp\left[\mathrm{i}\, kz - \frac{\rho^2}{w_0^2(1 + \mathrm{i}\, z/z_r)}\right] \left[P_x^+\left(\frac{x}{1 + \mathrm{i}\, z/z_r}, \frac{z}{1 + \mathrm{i}\, z/z_r}\right) + P_x^-\left(\frac{x}{1 + \mathrm{i}\, z/z_r}, \frac{z}{1 + \mathrm{i}\, z/z_r}\right)\right] \\ & \times \left[P_y^+\left(\frac{y}{1 + \mathrm{i}\, z/z_r}, \frac{z}{1 + \mathrm{i}\, z/z_r}\right) - P_y^-\left(\frac{y}{1 + \mathrm{i}\, z/z_r}, \frac{z}{1 + \mathrm{i}\, z/z_r}\right)\right] \end{aligned} \tag{35}$$

with $P_j^{\pm}(j,z)$ given by

$$P_j^{\pm}(j,z) = \exp\left(\frac{k}{2\,\mathrm{i}\, z}(w_{0j} \pm \mathrm{i}\, j)^2\right) \mathrm{erfc}\left(\sqrt{\frac{k}{2\,\mathrm{i}\, z}}(w_{0j} \pm \mathrm{i}\, j)\right). \tag{36}$$

As the longitudinal component is negligible in comparison with the x component, it is neglected within the paraxial approximation.[22]

3. Numerical calculations and analyses

Figure 1 represents the normalized intensity distribution of the SLG_{01} mode beam with different parameters in the source plane, where the normalized intensity is given by $(|E_x|^2 + |E_y|^2 + |E_z|^2)/(|E_x|^2 + |E_y|^2 + |E_z|^2)_{\max}$. The subscript max denotes taking the maximum of intensity. For comparison, the normalized intensity of the HG_{01} mode beam with the same f is also depicted in Fig. 1(d). The beam spot of the SLG_{01} mode beam is composed of two lobes and located at the y-axis. In the source plane, the beam spot of the SLG_{01} mode beam is smaller than that of the corresponding HG_{01} mode beam. The normalized intensity distributions of the SLG_{01} mode beam and the HG_{01} mode beam in the reference plane $z = 5z_r$ are depicted in Fig. 2. For comparison, parameters in subfigures (a)–(d) of Fig. 2 correspond to those in subfigures (a)–(d) of Fig. 1. In the nonparaxial regime, the divergence of the SLG_{01} mode beams is still larger than that of the corresponding HG_{01} mode beam.

Now, we quantitatively investigate the difference between the nonparaxial and the paraxial results. As the SLG_{01} mode beam depends on three parameters f, f_x, and f_y, we investigate the influence of these three parameters on the difference between the nonparaxial and the paraxial results.

First, an appropriate reference plane is to be selected. Figure 3 represents the normalized intensity distribution of the SLG_{01} mode beam in the difference reference planes. As $I(0, y, z)$ is independent of f_x and $I(x, 0, z)$ is equal to zero, the normalized intensity distribution in the section plane $y = x$ is examined. The reference planes are $z = z_r$, $5z_r$, and $15z_r$, respectively. The parameters used for the calculation are chosen as follows: $f = 0.2$, $f_x = 0.01$, and $f_y = 0.02$. The solid and the dotted curves correspond to the nonparaxial and the paraxial results, respectively. As shown in Fig. 3, the difference between the nonparaxial and the paraxial results is nearly independent of the axial propagation distance z. Therefore, the reference plane $z = 5z_r$ is used in the following calculations.

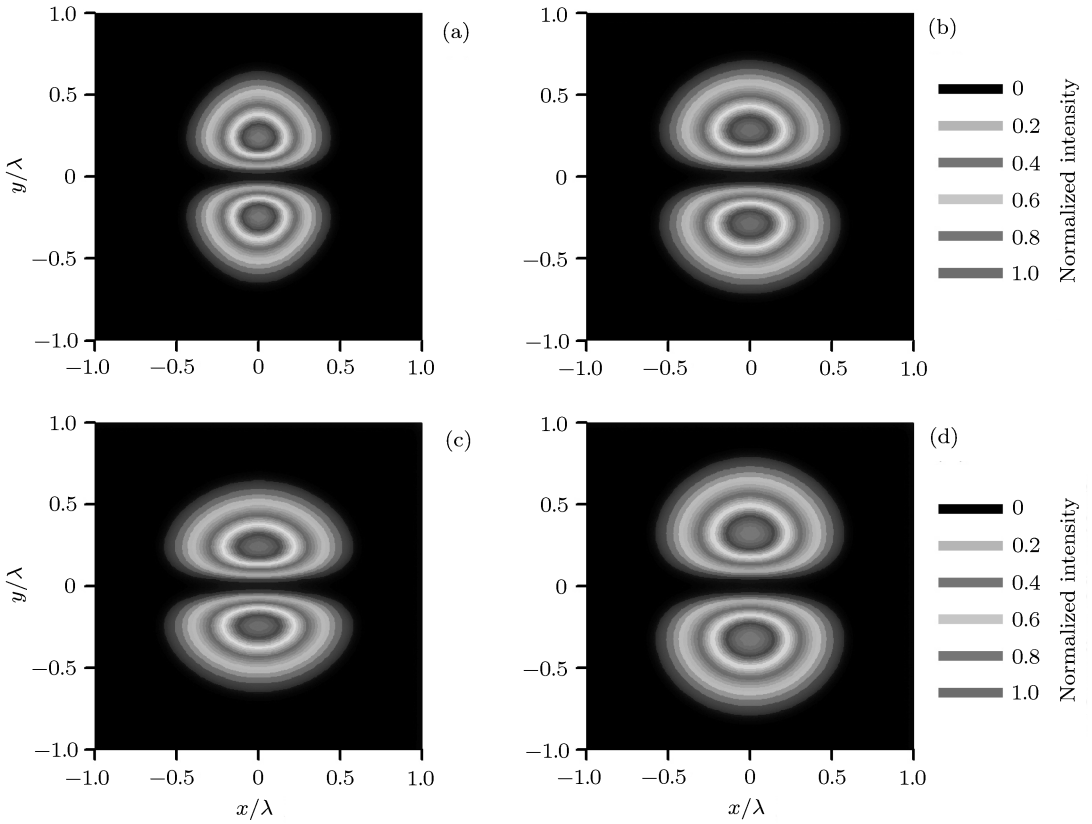


Fig. 1. The normalized intensity distributions of the SLG_{01} mode beam and the HG_{01} mode beam in the source plane $f = 0.35$. (a) SLG_{01} with $f_x = f_y = 0.35$; (b) SLG_{01} with $f_x = 0.1$ and $f_y = 0.2$; (c) SLG_{01} with $f_x = 0.01$ and $f_y = 0.35$; (d) HG_{01}.

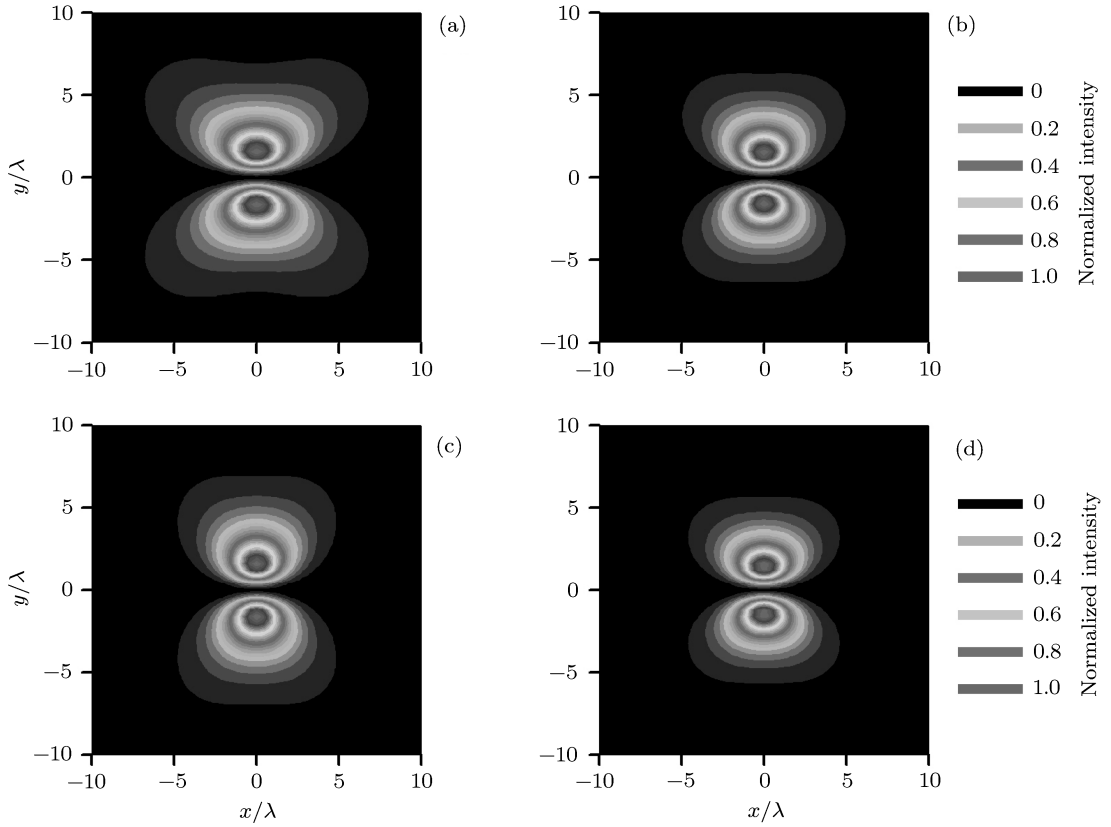


Fig. 2. The normalized intensity distributions of the SLG_{01} mode beam and the HG_{01} mode beam in the reference plane $z = 5z_r$, $f = 0.35$: (a) SLG_{01} with $f_x = f_y = 0.35$; (b) SLG_{01} with $f_x = 0.1$ and $f_y = 0.2$; (c) SLG_{01} with $f_x = 0.01$ and $f_y = 0.35$; (d) HG_{01}.

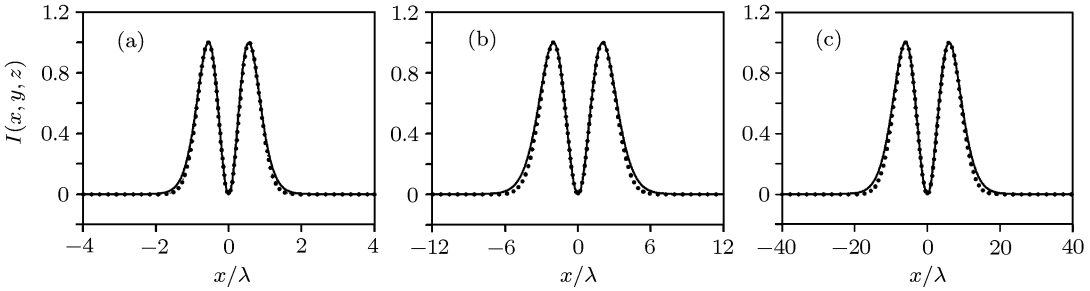


Fig. 3. The normalized intensity distribution of the SLG_{01} mode beam in the section plane $y = x$, $f = 0.2$, $f_x = 0.01$, and $f_y = 0.02$: (a) $z = z_r$; (b) $z = 5z_r$; (c) $z = 15z_r$.

Then, f_x and f_y are fixed, and we examine the influence of the parameter f on the difference between the nonparaxial and the paraxial results. For a Gaussian beam, the paraxial approximation condition is $w_0 \geq 2\sqrt{2}\lambda/\pi \approx 0.9\lambda$.[23] Accordingly, the case of w_0 being less than the wavelength is referred to as the nonparaxial case.[24] Here, the nonparaxial range denotes that the w_0, w_{0x}, and w_{0y} are values between 0 and λ. In other words, if f, f_x, and f_y are larger than 0.159, they are within the nonparaxial range; otherwise they are in the paraxial framework. In Fig. 4, f_x and f_y are kept to be 0.01 and 0.02, which denotes that they are both in the paraxial framework. The parameter f is a variable. $f = 0.35$, 0.2, and 0.1 in subfigures (a)–(c) of Fig. 4, respectively. When f is relatively large such as $f = 0.35$, the difference between the nonparaxial and the paraxial results is very distinct. As f decreases, the difference between the nonparaxial and the paraxial results also decreases. When f is small such as $f = 0.1$, the nonparaxial result is in good agreement with the paraxial result.

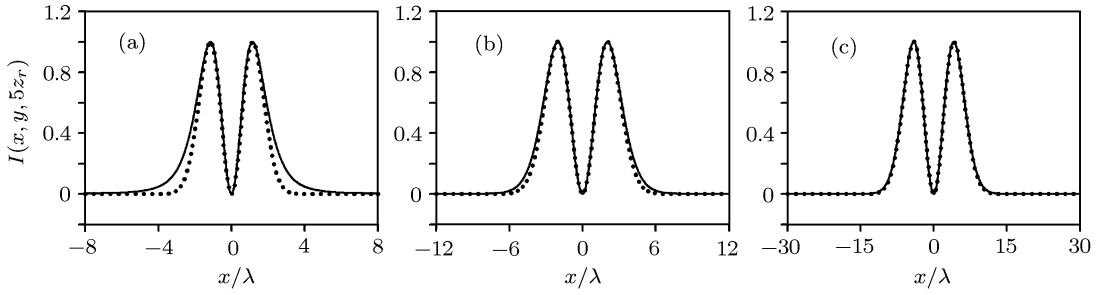


Fig. 4. The normalized intensity distribution of the SLG_{01} mode beam in the section plane $y = x$, the reference plane is $z = 5z_r$, $f_x = 0.01$ and $f_y = 0.02$: (a) $f = 0.35$; (b) $f = 0.2$; (c) $f = 0.1$.

Finally, the influences of the parameters f_x and f_y on the difference between the nonparaxial and the paraxial results are investigated and shown in Fig. 5. According to Fig. 4(c), f is set to be 0.1, $f_x = 0.5$ and $f_y = 0.02$ in Fig. 5(a). In Fig. 5(b), $f_x = 0.01$ and $f_y = 0.5$, whereas $f_x = f_y = 0.5$ in Fig. 5(c). Only one parameter of f_x and f_y is within the nonparaxial range; the difference between the nonparaxial and the paraxial results cannot be apparently detected. When the two parameters f_x and f_y are both within the nonparaxial regime, the difference between the nonparaxial and the paraxial results is noticeable. Therefore, the parameter f mainly determines the nonparaxiality of the SLG_{01} mode beam. When f is within the nonparaxial range or when f_x and f_y are both within the nonparaxial range, the SLG_{01} mode beam must be treated within the nonparaxial framework.

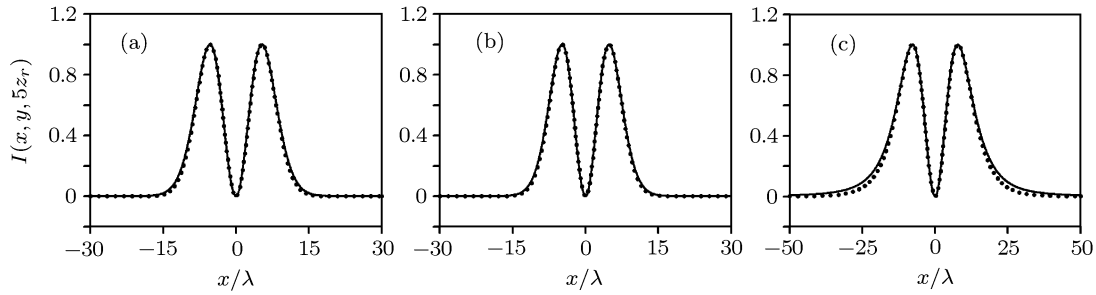


Fig. 5. The normalized intensity distribution of the SLG_{01} mode beam in the section plane $y = x$. The reference plane is $z = 5z_r$, $f = 0.1$: (a) $f_x = 0.5$ and $f_y = 0.02$; (b) $f_x = 0.01$ and $f_y = 0.5$; (c) $f_x = f_y = 0.5$.

To compare the nonparaxial propagation of the SLG_{01} and SLG_{00} mode beams, the normalized intensity distribution of the SLG_{00} mode beam in the section plane $y = x$ is depicted in Figs. 6 and 7. The parameters in subfigures (a)–(c) of Fig. 6 correspond to those in subfigures (a)–(c) of Fig. 4, respectively. The parameters in subfigures (a)–(c) of Fig. 7 are the same as those in subfigures (a)–(c) of Fig. 5. Through comparisons, we can find that the influences of the parameters f, f_x, and f_y of the SLG_{00} mode beam on the difference between the nonparaxial and the paraxial results are slightly smaller than those of the SLG_{01} mode beam.

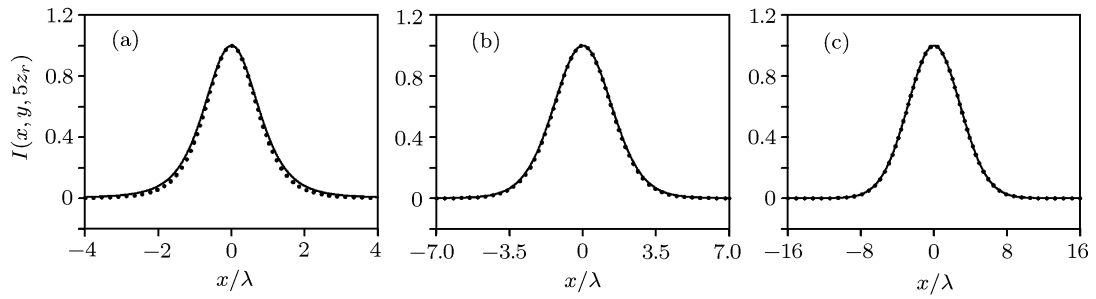


Fig. 6. The normalized intensity distribution of a SLG_{00} mode beam in the section plane $y = x$. The reference plane is $z = 5z_r$, $f_x = 0.01$ and $f_y = 0.02$: (a) $f = 0.35$; (b) $f = 0.2$; (c) $f = 0.1$.

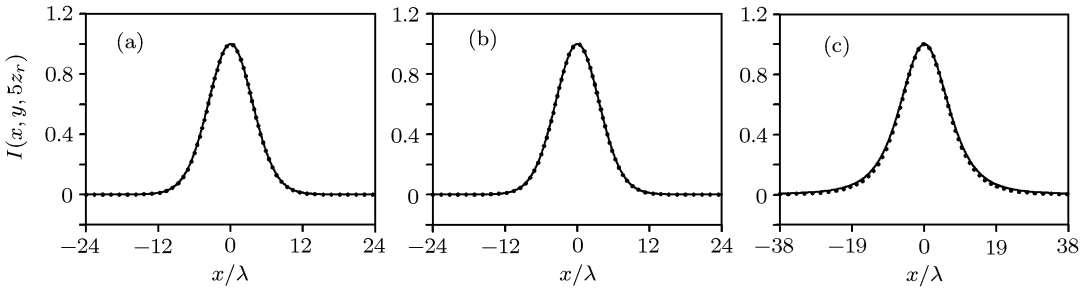


Fig. 7. The normalized intensity distribution of the SLG_{00} mode beam in the section plane $y = x$. The reference plane is $z = 5z_r$, $f = 0.1$: (a) $f_x = 0.5$ and $f_y = 0.02$; (b) $f_x = 0.01$ and $f_y = 0.5$; (c) $f_x = f_y = 0.5$.

4. Conclusions

Based on the vectorial Rayleigh–Sommerfeld integral formulae, the analytical nonparaxial propagation expression of the SLG_{01} mode is derived in free space. The far field expression and the scalar paraxial result are also treated with special cases of the general formulae. According to the derived formulae, the nonparaxial propagation properties of the SLG_{01} mode beam are illustrated and analysed with numerical examples. In the nonparaxial case, the divergence of the SLG_{01} mode beam is still larger than that of the HG_{01} mode beam. The parameter f mainly determines the nonparaxiality of the SLG_{01} mode beam. When f is within the nonparaxial range or when f_x and f_y are both within the nonparaxial range, the SLG_{01} mode beam must be treated within the nonparaxial framework. This research reveals the propagation behaviour of the SLG_{01} mode beam beyond the paraxial approximation and provides an approach to investigate the nonparaxial propagation of the SLG_{01} mode beam. The nonparaxial propagation of other SLG beams can be analysed by the same procedure.

References

[1] Naqwi A and Durst F 1990 *Appl. Opt.* **29** 1780
[2] Gawhary O E and Severini S 2006 *J. Opt.* A: *Pure Appl. Opt.* **8** 409
[3] Dumke W P 1975 *J. Quantum Electron.* **11** 400
[4] Zhou G Q 2008 *Appl. Phys.* B **93** 891
[5] Zhou G Q 2009 *Chin. J. Lasers* **36** 2326 (in Chinese)
[6] Zhou G Q 2009 *Chin. Phys.* B **18** 1853
[7] Zhou G Q 2008 *J. Opt. Soc. Am.* A **25** 2594
[8] Zhou G Q 2009 *Chin. Phys.* B **18** 2779
[9] Gawhary O E and Severini S 2007 *Opt. Commun.* **269** 274
[10] Zhou G Q 2008 *Acta Phys. Sin.* **57** 3494 (in Chinese)
[11] Zhou G Q 2009 *Appl. Phys.* B **96** 149
[12] Zhou G Q 2009 The high-order Lorentz–Gauss beams: super-Lorentzian-Gauss mode beams (submitted to *Opt. Lett.*)
[13] Agrawal G P and Pattanayak D N 1979 *J. Opt. Soc. Am.* **69** 575
[14] Wünsche A 1992 *J. Opt. Soc. Am.* A **9** 765
[15] Zeng X, Liang C and An Y 1999 *Appl. Opt.* **38** 6253
[16] Seshadri S R S 2003 *Opt. Lett.* **28** 595
[17] Luneberg P K 1966 *Mathematical Theory of Optics* (Berkeley: University of California Press)
[18] Mei Z R and Zhao D M 2007 *Opt. Express* **15** 11942
[19] Ciattoni A, Crosignani B and Porto P D 2002 *Opt. Commun.* **202** 17
[20] Mei Z R and Zhao D M 2008 *J. Opt. Soc. Am.* A **25** 537
[21] Gradshteyn I S and Ryzhik I M 1980 *Table of Integrals, Series, and Products* (New York: Academic Press)
[22] Chen C G, Konkola P T, Ferrera J, Heilmann R K and Schattenburg M L 2002 *J. Opt. Soc. Am.* A **19** 404
[23] Nemoto S 1990 *Appl. Opt.* **29** 1940
[24] Martínez-Herrero R, Mejías P M and Bosch S 2008 *Opt. Commun.* **281** 3046